**NASA TECHNICAL MEMORANDUM**

NASA TM X-73,171

NASA TM X-73,171

# INVESTIGATING COMPLEX AERODYNAMIC FLOWS WITH A LASER VELOCIMETER

K. L. Orloff, V. R. Corsiglia, J. C. Biggers,
and T. W. Ekstedt

Ames Research Center
and
Ames Directorate
U.S. Army Air Mobility R&D Laboratory
Moffett Field, California 94035



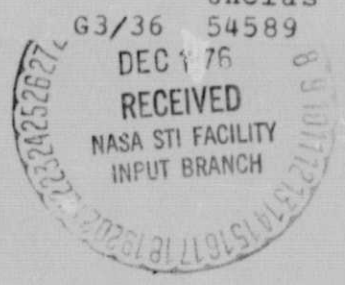


October 1976

| 1. Report No. | 2. Government Accession No. | 3. Recipient's Catalog No. |
|---|---|---|
| TM X-73,171 | | |

| 4. Title and Subtitle | 5. Report Date |
|---|---|
| INVESTIGATING COMPLEX AERODYNAMIC FLOWS WITH A LASER VELOCIMETER | 6. Performing Organization Code |

| 7. Author(s) | 8. Performing Organization Report No. |
|---|---|
| K. L. Orloff, V. R. Corsiglia, J. C. Biggers,* and T. W. Ekstedt** | A-6765 |

| 9. Performing Organization Name and Address | 10. Work Unit No. |
|---|---|
| NASA Ames Research Center and Ames Directorate, U.S. Army Air Mobility R&D Laboratory, Moffett Field, CA 94035 | 505-10-21 |
| | 11. Contract or Grant No. |

| 12. Sponsoring Agency Name and Address | 13. Type of Report and Period Covered |
|---|---|
| National Aeronautics and Space Administration Washington, D. C. 20546 and U.S. Army Air Mobility R&D Laboratory, Moffett Field, CA 94035 | Technical Memorandum |
| | 14. Sponsoring Agency Code |

15. Supplementary Notes

*Ames Directorate, U.S. Army Air Mobility R&D Laboratory.
**At University of California, Davis, California 95616.

16. Abstract

This paper discusses the application of the laser velocimeter in the study of two highly complex aerodynamic flows. In the first experiment, the laser velocimeter has been used with frequency tracking electronics to survey the multiple vortex wake structure behind a model of a large jet transport. The second application is to the study of the induced instantaneous inflow velocities near the blades of a model helicopter rotor; counter-type processing was used in these measurements. In each experiment, the data output channels of these processors were handled in an on-line fashion, including both velocity computations and the plotting of fully reduced data.

| 17. Key Words (Suggested by Author(s)) | 18. Distribution Statement |
|---|---|
| Laser velocity measurements<br>Signal processing electronics<br>Aerodynamic flows | Unlimited<br>STAR Category - 36 |

| 19. Security Classif. (of this report) | 20. Security Classif. (of this page) | 21. No. of Pages | 22. Price* |
|---|---|---|---|
| Unclassified | Unclassified | 30 | $3.75 |

*For sale by the National Technical Information Service, Springfield, Virginia 22161

# INVESTIGATING COMPLEX AERODYNAMIC FLOWS WITH A LASER VELOCIMETER

K. L. Orloff, V. R. Corsiglia, J. C. Biggers,* and T. W. Ekstedt**

Ames Research Center
and
Ames Directorate
U.S. Army Air Mobility R&D Laboratory

## SUMMARY

This paper discusses the application of the laser velocimeter in the study of two highly complex aerodynamic flows. In the first experiment, the laser velocimeter has been used with frequency tracking electronics to survey the multiple vortex wake structure behind a model of a large jet transport. The second application is to the study of the induced instantaneous inflow velocities near the blades of a model helicopter rotor; counter-type processing was used in these measurements. In each experiment, the data output channels of these processors were handled in an on-line fashion, including both velocity computations and the plotting of fully reduced data.

## INTRODUCTION

For some time now researchers have found that the optical configuration of the laser velocimenter (LV) to be used can be dictated by the physical characteristics of a particular flow facility (wind tunnel, water flow, etc.). When optical access to the flow is limited, or a clear view of the focal volume is for some reason not possible in the forward scatter direction, the backscatter arrangement is usually chosen, and the scientist must be satisfied with a reduced Mie scattering cross section (ref. 1). Also, where the probe volume must be translated over a substantial distance or at high speed, the confocal backscatter arrangement has usually been chosen, and optical, telescopic-type scanning has been used.

Similarly, the choice of LV signal processing electronics cannot be made without giving sufficient consideration to the flow field that is to be measured and the expected characteristics of the velocimeter signals (ref. 2). A flow which is unsteady or exhibits a high turbulence intensity can often cause difficulty when spectrum analysis techniques are used. Problems can also be encountered when processing LV signals generated by a flow that is of a transient or periodic nature. Also, the processor may be required to operate with a highly variable signal-to-noise ratio such as might result from a spatially scanning optical system, or from variations in seeding density or particle size. Additionally, a spatially scanning optical system can itself be the source of transient signals that must be accommodated by the signal processor. In short, the signal processor must be chosen to be compatible with the signals that will result from the flow to be studied.

*Ames Directorate, U.S. Army Air Mobility R&D Laboratory.
**At University of California, Davis, California 95616.

One must also consider the requirements of data acquisition and data reduction. Laser velocimeter investigations of highly complex aerodynamic flows can be substantially augmented by rapid, on-line, data reduction and presentation; this can generate valuable technical feedback that may prove useful during the course of the experiment.

It is the purpose of this paper to discuss the application of the laser velocimeter in two highly complex aerodynamic flow situations. Frequency tracking and period counting signal processing electronics were used in these studies, and they are discussed with respect to the complex flow situation in which they were found to be respectively applicable. In both of these experiments, the data output channels of the processors have been handled in an on-line fashion, including both velocity computations and the plotting of fully reduced data.

The laser velocimeter which was used for these experiments (fig. 1) was developed at the Ames Research Center specifically for subsonic measurements in the Ames 7- by 10-Foot Wind Tunnel (ref. 3). It is a crossed-beam, on-axis backscatter instrument that uses two of the colors emitted from an argon-ion laser for the simultaneous measurement of orthogonal velocities. It also incorporates a means for optically translating the focal volume along the optical axis.

## VORTEX WAKE VELOCITY SURVEYS

The laser velocimeter has proven itself to be an important research tool in the study of aircraft wake vortices. Because it is a nonintrusive probe, it is ideally suited to making measurements in this type of flow which is known to be sensitive to disturbances.

Early laser velocimeter studies of vortex wakes at Ames have utilized spectrum analyzers as the primary signal processing electronics (ref. 4). This type of processing has, however, recently been replaced by a Raytheon Model 15/55G Two-Channel Frequency Tracker. The laser velocimeter has been used with this frequency tracker to survey the wake structure behind a Boeing 747 model installed in the test section of the Ames 7- by 10-Foot Wind Tunnel (fig. 2). A model configuration was studied that shows promise of producing a less intense wake structure. In this configuration, the inboard flaps of the model are deflected 30° while the outboard flaps remain retracted.[1] Unlike the simple vortex pair structure, which is generated by an unflapped wing, this flapped configuration generates a considerably more complex multiple vortex wake. As a result, the velocity field is no longer adequately defined by a single linear optical scan of the velocimeter as previously reported for the simple wake of a straight rectangular wing (ref. 4). Instead, the entire wake velocity field must be mapped in a

[1]The Conventional landing situation has both inboard and outboard flaps deployed by 30°.

cross-section plane of the wind tunnel. Such a mapping is accomplished by making optical traverses with the velocimeter at a number of elevations in the wind tunnel. Figure 3 shows a light-slit photograph that visualizes this wake at 1.5 wing spans behind the model (the location at which all data were taken). The discussion of data acquisition and reduction later in this section will make reference to the horizontal line traverses taken through vortex pairs as noted in figure 3.

Since the wake pattern was not stationary in the wind tunnel, the focal volume was traversed across the flow in approximately 3 sec in order to encompass the area of interest and still retain the detail near the vortex cores. An optical scan of nearly 2 m was required. Particulate scattering material was introduced into the diffuser section of the wind tunnel by means of a mineral oil aerosol generator. Recirculation of the air around the wind tunnel circuit then provided a light concentration of the aerosol, and velocimeter data could be gathered throughout the test section. The vortical patterns in the flow, however, created a centrifugal action which centrifuged out the particles. This resulted in a slightly variable signal-to-noise ratio with an occasional complete loss of signal as the focal volume was translated optically across the wind tunnel. During the traverse, a widely varying signal-to-noise ratio, caused by the spherical aberrations of the lens system, compounded the problem. This velocimeter is presently being operated with a "doublet" transmitting-receiving lens system in an attempt to minimize the effects of these aberrations as the effective focal length of the system is varied (ref. 5).

In this experiment, period counting electronics were found to be unusable due to a lack of automatic gain control (AGC). The frequency tracker, on the other hand, was found to lock on and track whenever the signal-to-noise ratio was 4 dB or greater. An automatic gain control threshold is provided on this instrument to optimize the tracker response for variable input noise level and signal level.

Another feature of the tracker is that, when in the automatic mode, it is not necessary to "tune" the voltage controlled oscillator (VCO) until signal is acquired before initiating tracking. Whenever a signal is present above a preset threshold and within the bandwidth of the tracker (100 kHz), the tracker will lock on and track this signal automatically in a maximum time of 3 msec. If the signal should "drop out," a variable time delay "hold" mode, adjustable between 0.1 msec and 100 msec, keeps the loop locked. After this time, if the signal does not reappear, an automatic "sweep" mode searches for the signal over the entire instrument range (0-15 MHz) in approximately 5 msec.

This automatic sweep and lock-on feature of the tracker was important during optical traverses of the Boeing 747 wake. As already noted, there was a complete loss of signal occasionally as the focal volume penetrated a vortex core. When the signal would reappear, the signal-to-noise level was often quite different, and the frequency often a considerable distance from the "held" value. The tracker was then required to unlock, search, lock on, and

track this new signal. The instrument was able to operate satisfactorily under these conditions.

The difference in velocity between the regions far from vortex centers and those near the vortices, produced signal frequencies that varied over a wide range, typically from about 0.5 MHz to 5.0 MHz, in a short period of time. The frequency tracker was able to track adequately under these conditions since it utilizes only a single broad frequency range that extends from about 0.05 MHz to about 15 MHz, with a slew rate in excess of 20 MHz/sec.

The data acquisition apparatus for these wake vortex experiments is presented schematically in figure 4. The d.c. output (low pass below 40 Hz) from each tracker channel was recorded continuously as the focal point of the velocimeter was traversed across a selected portion of the wind tunnel. The transient capture device (TCD) is a high speed data acquisition system that digitizes analog signals and is capable of multiplexing up to four analog inputs. The sampling rate is variable, and in these experiments was set such that the 4096-word (10-bit resolution) memory would fill during the time the focal point was accomplishing a single traverse of the flow. These data were stored in core memory and, if desired, could be transferred to an integral magnetic tape cassette capable of storing as many as 35 records. In this fashion, any one of these records could later be recalled from the tape back into the memory and then reduced after a series of line surveys had been completed. These surveys were taken at a sufficient number of elevations to completely specify the wake structure.

Figure 5 shows a 4096-word digital TCD record of a traverse through the wake at the elevation of the inboard flap vortices (refer to fig. 3). In these experiments, directional sensitivity was accomplished by rotating the LV optical system by nearly 40° about the optical axis, thus biasing both channels of the velocimeter with a component of the free-stream velocity. The trend of decreasing frequency with increasing scan distance is caused by a decrease in the included cross-beam angle as the focal point moves across the wind tunnel. The spatially compressed appearance of the wake structure on the right-hand side of the centerline is due to the nonlinear scanning speed of the focal point for a constant motion of the scanning lens element. Each signal crossover of the two tracker signals on this record indicates the presence of a vortex.

Figure 6 is a digital record for a traverse through the strong outboard flap vortex pair. Notice that the frequency tracker was able to successfully remain locked as the focal volume passed through the high velocity gradients encountered near the centers of these vortices. Figure 7 is a record of a traverse through the tip vortex pair. The velocity defect created by the strut, upon which the model was mounted, is noted to be coincident with the geometrical centerline in the wind tunnel.

An important property of the LV processed signal is its linear relationship to the velocity component sensed, without the need for an elaborate calibration. It was feasible, therefore, to implement prompt data reduction with a complete, on-line presentation of the velocity profiles. Since the LV

optical system is capable of sensing two velocity components simultaneously, one can generate an on-line display of, in the case of wake vortices, both the streamwise and the vertical velocity distributions along the optical scanning direction.

After a desired wake traverse record has been transferred from the magnetic tape into the core memory of the TCD, this "raw" data is then processed and reduced as indicated in figure 8. The rate of parallel digital output is controlled externally by stopping and starting a digital clock. The software instructs the programmable desk calculator to interrogate the interface for a "word" of data. This request then causes the interface to generate an "execute" pulse which starts the digital clock. These clock pulses tell the TCD to serially load a data "word." When all 10 bits have been loaded, the TCD generates a "strobeout" pulse which simultaneously stops the digital clock and informs the interface that new data are ready for transfer. Three consecutive words (two frequencies, one position) are loaded into the calculator in this manner. The program uses the binary position word to compute the tunnel location of the focal volume and the cross-beam intersection angle; the velocities are then computed in the rotated coordinate frame. After performing a coordinate rotation back to the streamwise and vertical directions, the calculator transfers these values to a digital flatbed plotter which plots the two velocities versus the position of the focal point. This entire procedure is then repeated for another set of three data points.

Figures 9, 10, and 11 show the processed, reduced, and plotted data corresponding to figures 5, 6, and 7, respectively. In figure 10, the fact that the traverse was nearly perfectly centered on the left vortex (as evidenced by the steep velocity gradient) while missing the center of the right vortex is to be expected if there is even a slight motion of the vortex wake pattern during a traverse. The streamwise profile provides the scientist with information related to the drag of the generating model; the vertical distribution provides a measure of the strength of the wake and therefore some indication of the hazard it would present to an encountering aircraft.

## HELICOPTER ROTOR INFLOW MEASUREMENTS

The flow field generated by a helicopter rotor is extremely complex and difficult to analytically predict or experimentally measure. The vortices that are shed from the blade tips produce high velocity gradients within the flow. High blade loadings are experienced by blades which then encounter these regions of high shear. Figure 12 illustrates the convection by the free stream of the vortices from the blade tips for a forward flight condition that has been tested (refs. 6 and 7). The rotor wake may be visualized as a skewed contracting cylinder, bounded by the tip vortices. The epicycloid of figure 12 is the instantaneous location of the two tip vortices for the first four quadrants of the rotor rotation.

In recent years, several investigations (refs. 6-9) have applied laser velocimeters to the problem of measuring the complex helicopter rotor flow field. Reference 6 contains a brief history of rotor flow field measurements and indicates the reasons for using a laser velocimeter.

The objective of the LV investigation of the rotor flow fields reported here is to define accurately the velocity structure around the rotor blade at the instant the blade is passing through a specified azimuth position. It is the *instantaneous* velocity that must be measured if detailed blade aerodynamics are to be understood. Additionally, if the flow is surveyed in such a manner that these instantaneous velocities are measured along a rectangular path enclosing the airfoil (fig. 13), it is possible to determine the local value of the circulation by computing the line integral of the velocity along this path. The local aerodynamic loading on the blade is then directly related to this circulation.

For this investigation, a two-bladed teetering rotor, 2.13 m (7 ft) in diameter, was operated at a tip speed ratio of $V/\Omega R = 0.18$ in a 7- by 10-ft wind tunnel. Again, the LV optical package was tilted abou the optical axis (by about 15°) to obtain some degree of directional sensitivity. Figure 14 shows the rotor operating in this wind tunnel with the laser beams being projected into the test section from the observation window on the left.

Clearly, the extremely rapid time variation of this type of flow at any specified point near the rotor disk precludes the use of conventional frequency tracking or spectrum analyzer systems. More exactly, the transient flow structure associated with the passage of the blade occurs in a characteristic elapsed time of approximately 5 msec (at 300 rpm). Hence, even if frequency tracking electronics could operate at such a frequency slew rate, it is doubtful that an adequate density of scattering particles could be generated to provide a sufficiently continuous signal to represent accurately the details of the transient flow. It was, in fact, determined that the frequency tracker, even with the automatic sweep feature, was not able to resolve the detailed structure around the blade to the degree required in this experiment. In this type of flow it was therefore necessary to use counter-type signal processors to detect the instantaneous value of the fringe crossing frequency.

Two methods have been developed that utilize counter-type processors for these measurements, both of which rely upon the periodicity of the flow as a prerequisite. The first method attempts to reconstruct the periodic velocity distribution at a fixed point in the wind tunnel. This can be accomplished by recording the analog output of the processor for many rotations; several of these time histories are then superimposed to obtain an average profile. Such a technique has been successfully applied and is discussed in reference 7. If, however, the instantaneous spanwise loading distribution on the rotor blade is to be determined, then all of the data must be obtained when the blade is at a specified azimuth. For this type of measurement, it is clear that time histories as a function of blade azimuth are not adequate (except in the hover condition). The second method, which was used in the experiment reported here, is based on the following considerations.

The periodicity of the flow to be measured and the statistical nature of the LV signal suggest that one might "strobe" the data processing system to the periodicity of the flow. Data are only accepted once per revolution during a short "data window"; this "window" is open only when the blade is at a prescribed azimuth. In this manner, the strobing technique merely requires that one wait for particles to be in the fringe volume at the right time (while the "window" is open).

A block diagram of the signal processing equipment is given in figure 15. This data system is an improved version of that described in reference 6. To perform the strobing, a once-per-revolution signal from the rotor was used to trigger a pulse generator. The pulse generator was adjusted to produce a pulse width corresponding to 0.060 percent of one revolution, the time for the blade tip to travel 3.8 percent of the blade chord (0.22° of azimuth). Thus, in the data presented here, velocities were only measured when the rotor azimuth was 90° ± 0.11° (perpendicular to the tunnel free-stream flow).

The "data ready" pulse from the processor (1 μsec) is used for two purposes. It indicates to the interface that there is new information available at the input. Since the duration of this input control signal is required to be at least 5 μsec, a pulse stretcher is employed. Upon receiving this stretched pulse, the interface returns an "inhibit" command to the processor to hold the current value while it is being transferred to the calculator. When transfer has been completed, a signal is returned to the interface to reset the inhibit and allow the counter to continue processing. The time for transfer of the data from the interface to the calculator is 5 msec. Secondly, the "data ready" pulse is used to trigger an oscilloscope that is used to monitor the quality of the signals being processed (not shown on fig. 15). Actually, all that can be seen is the remainder of the signal after the required eight cycles of signal have been processed; this monitoring method does not work, of course, for signals where only the minimum number of required cycles are present.

The digital output of the counter-type processor is binary while the interface is set up for binary coded decimal (BCD). By connecting the binary registers three at a time to the three lower bits of the BCD registers, the counter output was converted to an octal coding. The interface transferred this octal number to the electronic calculator where a subroutine program converted the number to the base 10. The software instructed the system to multiplex the data acquisition for the five interfaces. The programmable calculator computed the velocities based on the counter outputs, collected a prescribed number of samples, performed a statistical analysis on the samples, rotated the coordinates, and then transferred the results to the digital plotter. The focal volume was then moved along the rectangular path by an incremental distance (determined by the resolution desired) and the acquisition scheme repeated. In this manner, the streamwise and vertical (downwash) velocity distributions were determined along each portion of the path shown in figure 13. Thus, the calculator and the plotter were important elements for the on-line data system used in this experiment.

The lift distribution on a helicopter rotor blade is usually measured using surface pressure transducers buried in the blade. Measurements can thus be made only at radial locations where the transducers have been placed. In the results presented here, the radial distribution of lift was obtained by measuring the distribution of bound vorticity on the blade (the line integral of the velocity). These measurements could be made at virtually any point along the blade. The LV was used to obtain the velocities along these closed paths enclosing the airfoil at various radial stations. These velocities were then integrated to find the circulation at each station. The circulation for a closed path is given by

$$\Gamma = \oint \vec{V} \cdot d\vec{s}$$

where $V$ is the total velocity vector and $d\vec{s}$ is an element of the path. For the rectangular path of figure 13, the calculation simplifies to

$$\Gamma = \int_1^2 u\,dx + \int_2^3 w\,dz + \int_3^4 u\,dx + \int_4^1 w\,dz$$

The data acquisition rate in this experiment was limited by the data transfer rate into the calculator. As a result, to obtain data along any of the paths indicated above (consisting of about 50 points) required approximately 1 hr. It is anticipated that this time could be reduced by perhaps a factor of four by replacing the calculator with a minicomputer having direct input wires from the processors.

Figure 16 presents a typical on-line plot of the distribution of the velocities above the blade (path 1-2). The effects of the bound vorticity are quite clear: the streamwise velocity above the airfoil is accelerated, and the vertical velocity is upward ahead of the airfoil and downward behind it. The effect of the airfoil thickness is clearly shown by the peak in the vertical velocity near the leading edge, as expected. Figure 17 is a velocity survey behind the blade (path 2-3), and the wake momentum deficit is obvious. Figure 18 presents the velocity profiles below the blade (path 3-4); the retardation of the flow is apparent near the leading edge. The structure in figure 18 is somewhat different from what one would expect to obtain in the case of a fixed wing due to the proximity of the tip vortex that was shed from the preceding blade. Figure 19 is a plot of the velocities ahead of the blade (path 4-1).

The circulation is calculated from an integration of the profiles in figures 16 through 19 according to the formula given above. When this is done at a number of spanwise locations, the load distribution is determined; this distribution is presented in figure 20.

## CONCLUSIONS

Two experimental applications of the laser velocimeter have been described. In both of these applications, the velocimeter has been

successfully used to perform diagnostics in a highly complex aerodynamic flow. The optical system, and also the dynamic characteristics of the fluid flow, were found to place certain requirements upon the signal processing electronics. Both frequency tracking and period counting signal processors were found to be applicable.

In the future, there will certainly be other complex flows to which laser velocimetry will be applied. At present there does not appear to be a signal processor that can be classified as universal for the requirements of all flows. Until such a processor is developed, the scientist must carefully evaluate the anticipated characteristics of the LV signal and choose an appropriate processor.

## REFERENCES


1. Meyers, J. F.: Investigation of Basic Parameters for the Application of a Laser Doppler Velocimeter. AIAA Paper 71-288, March 1971.

2. Meyers, J. F.; and Feller, W. V.: Processing of the Laser Doppler Velocimeter Signals. Paper presented at the Fifth International Congress on Instrumentation in Aerospace Simulation Facilities, Pasadena, CA, Sept. 1973.

3. Grant, G. R.; and Orloff, K. L.: Two-Color Dual-Beam Backscatter Laser Doppler Velocimeter, Applied Optics, vol. 12, Dec. 1973.

4. Orloff, K. L.: Trailing Vortex Wind-Tunnel Diagnostics with a Laser Velocimeter, J. Aircraft, vol. 11, no. 8, Aug. 1974.

5. Orloff, K. L.; and Biggers, J. C.: Laser Velocimeter Measurement of Developing and Periodic Flows. Paper presented at the International Workshop on Laser Velocimetry, Purdue Univ., March 1974.

6. Biggers, J. C.; and Orloff, K. L.: Laser Velocimeter Measurements of the Helicopter Rotor-Induced Flow Field, J. American Helicopter Soc., vol. 20, no. 1, Jan. 1975.

7. Biggers, J. C.; Chu, S.; and Orloff, K. L.: Laser Velocimeter Measurements of Rotor Blade Loads and Tip Vortex Rollup. Paper presented at the 31st Annual National Forum of the American Helicopter Society, Washington, D.C., May 1975. (Preprint No. 900)

8. Sullivan, J. P.: An Experimental Investigation of Vortex Rings and Helicopter Wakes Using a Laser Doppler Velocimeter, M.I.T. Aerophysics Laboratory TR-183, June 1973.

9. Landgrebe, A. J.; and Johnson, B. V.: Measurement of Model Helicopter Rotor Flow Velocities with a Laser Doppler Velocimeter, Tech. Note, J. American Helicopter Soc., vol. 19, no. 3, July 1974.

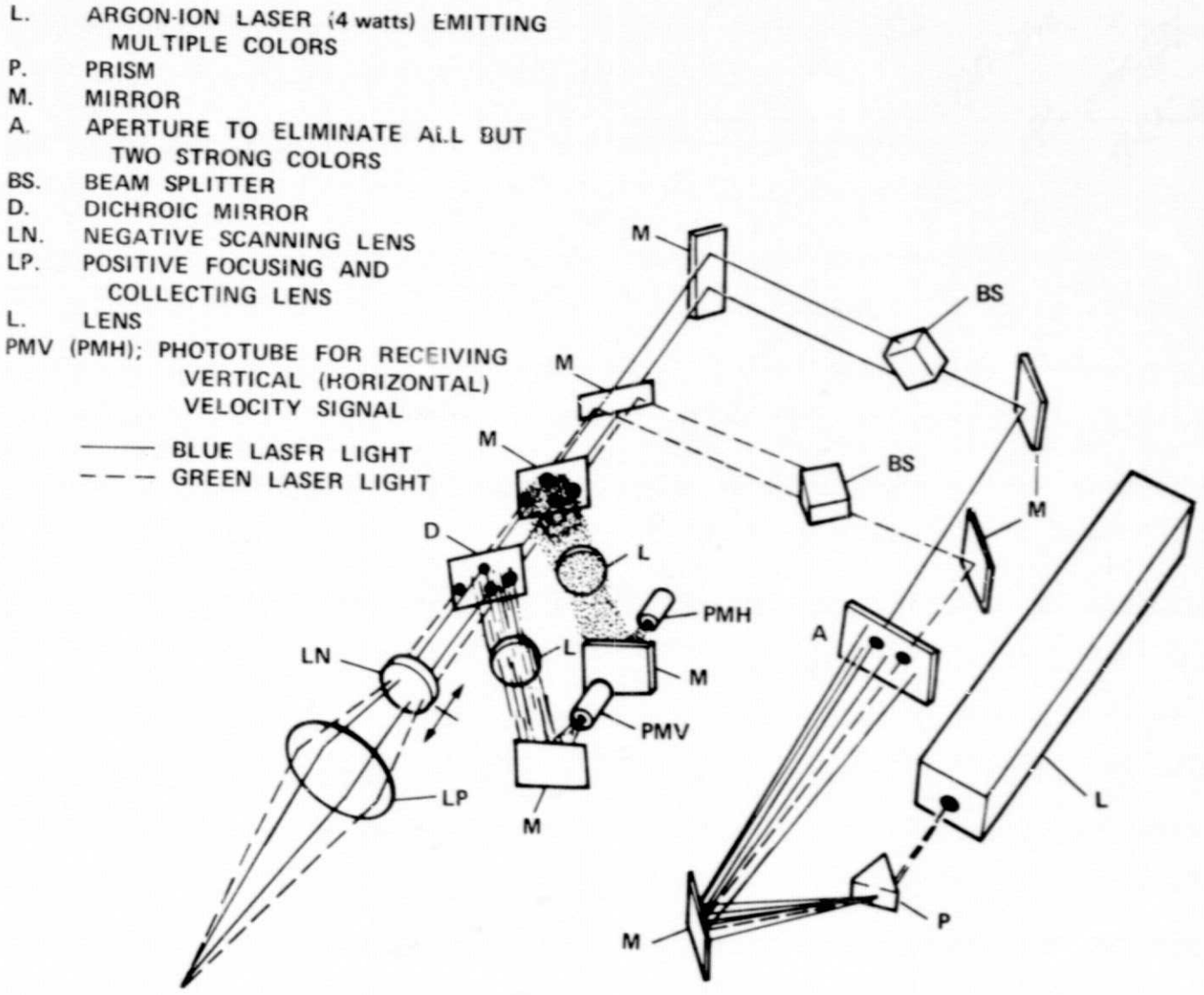


Figure 1.- Schematic diagram of two-color laser velocimeter.

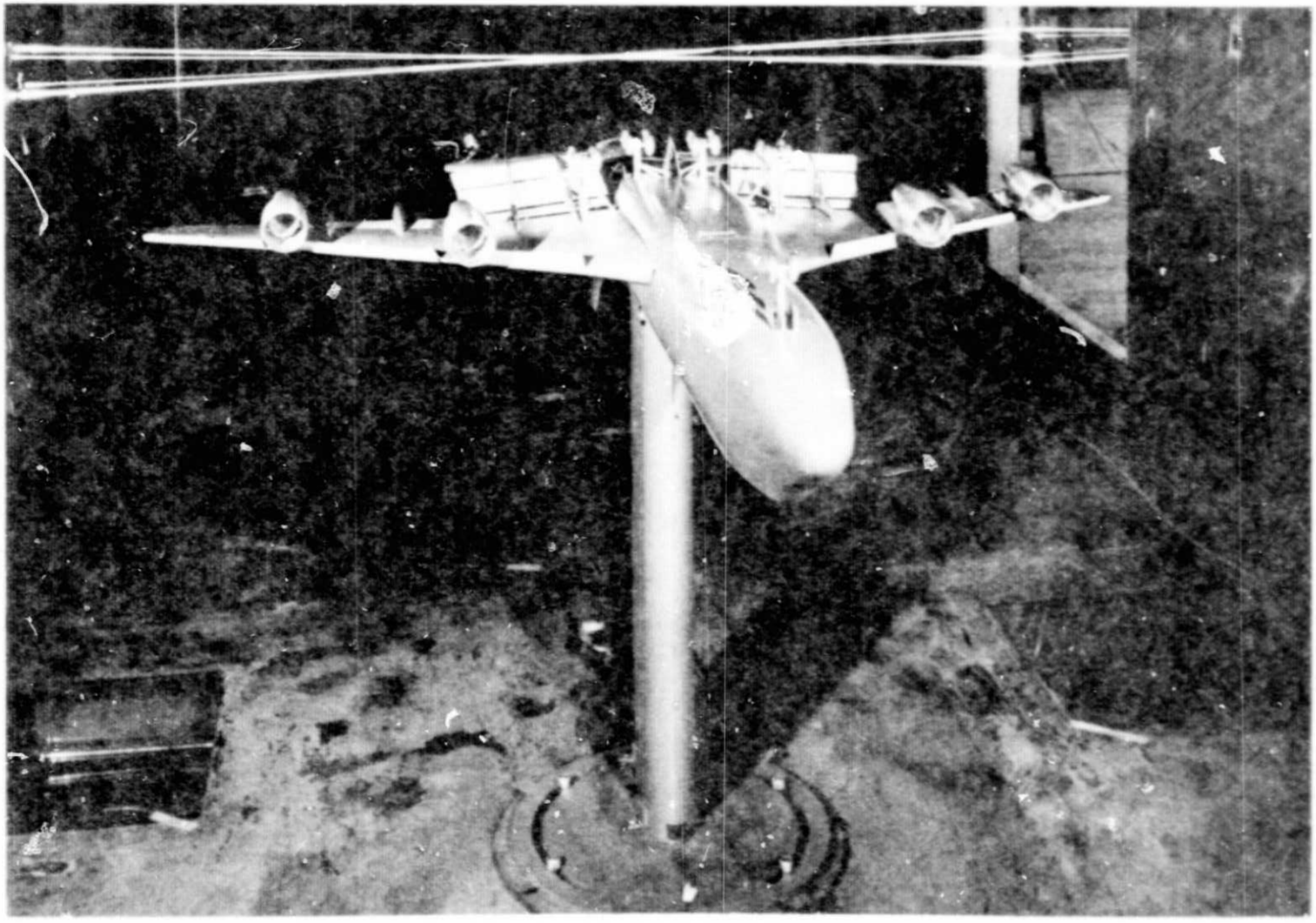

Figure 2.- Model of Boeing 747 installed in Ames 7- by 10-Foot Wind Tunnel. Model is mounted in the inverted position so that the strut wake will not interfere with the fluid dynamics associated with the flaps and landing gears. The laser beams pass behind the model at approximately 1.5 wing spans (3 m) aft of the trailing edge of the wing.

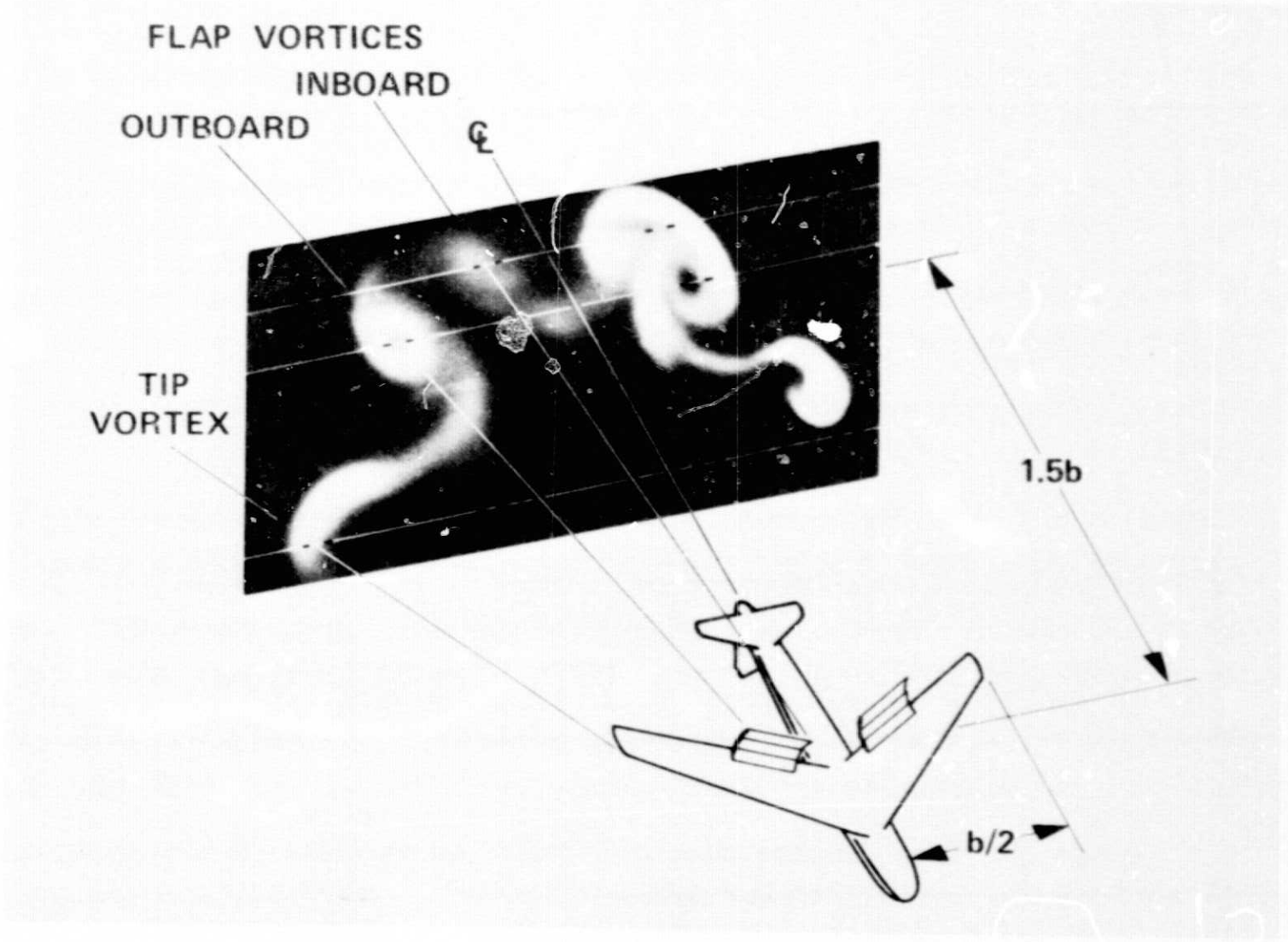


Figure 3.- Light-slit photograph of the vortex wake structure generated by the flap configuration shown in figure 1. Elevation lines are noted through vortex pairs which are shed from the wing.

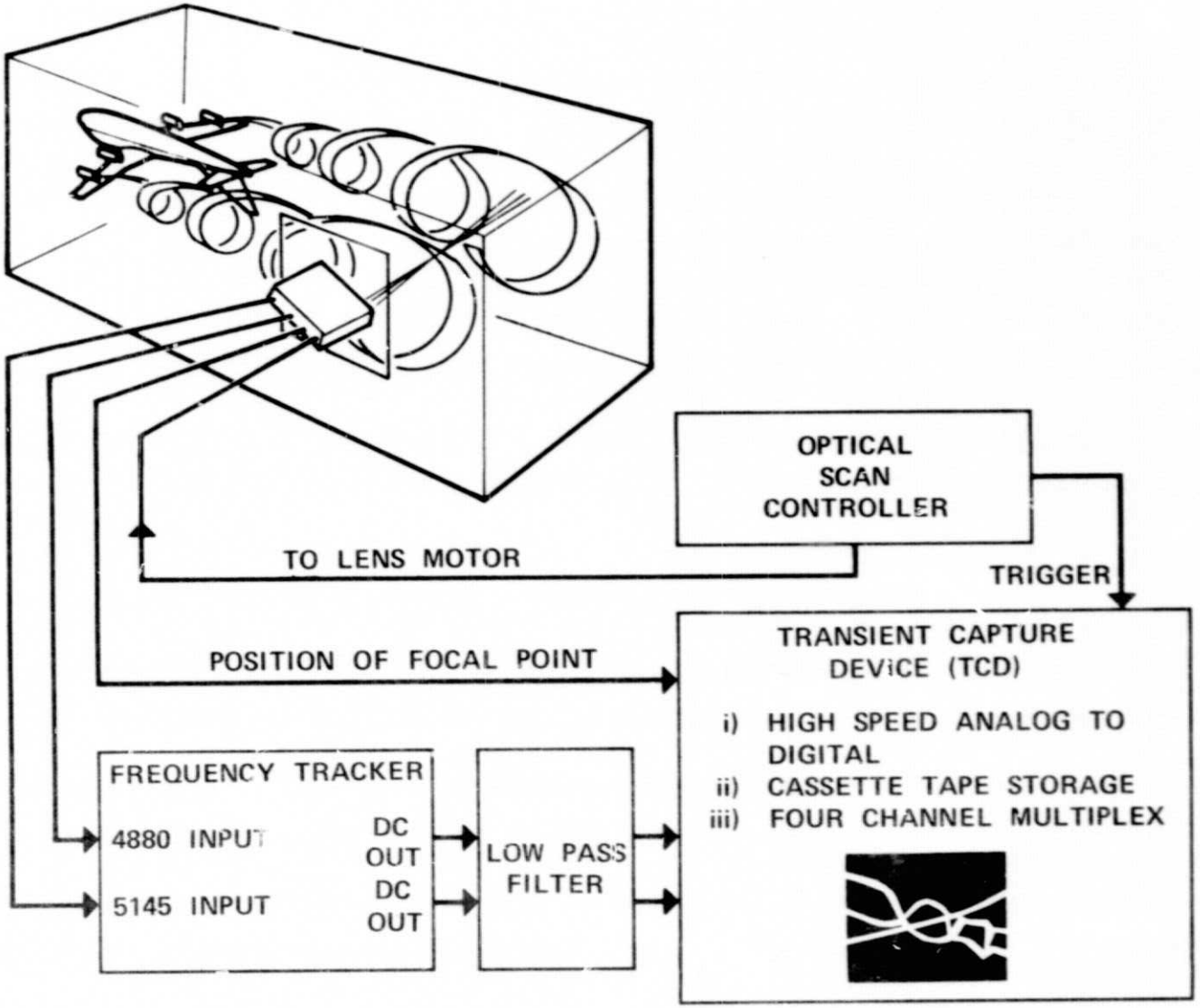


Figure 4.- Data acquisition schematic for Boeing 747 wake vortex experiment.

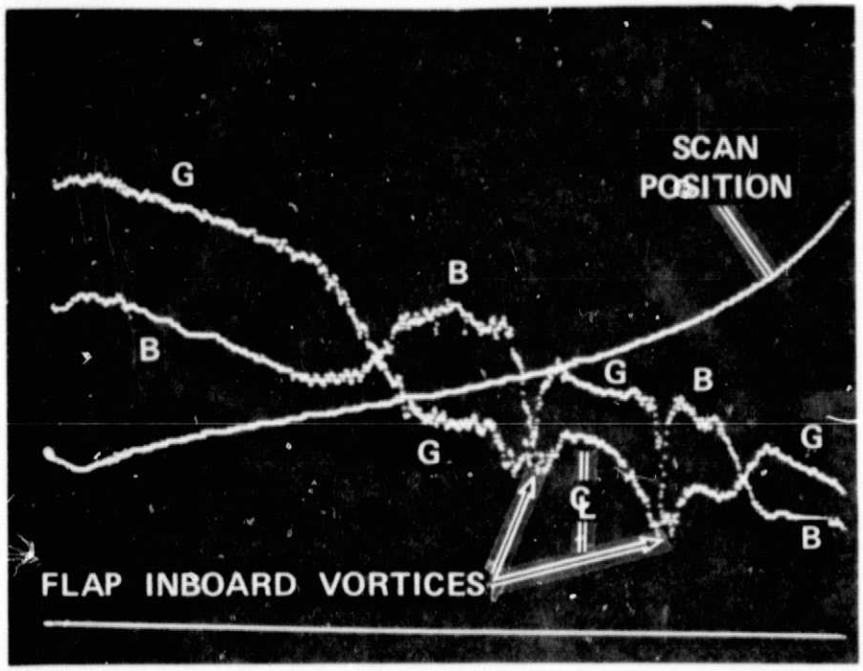


Figure 5.- Boeing 747 wake TCD record showing scan position of the focal point, centerline of the wind tunnel, and the tracker outputs (low pass below 40 Hz) corresponding to the blue (B) and green (G) channels of the velocimeter. This survey is through the flap inboard vortex pair as indicated in figure 2.

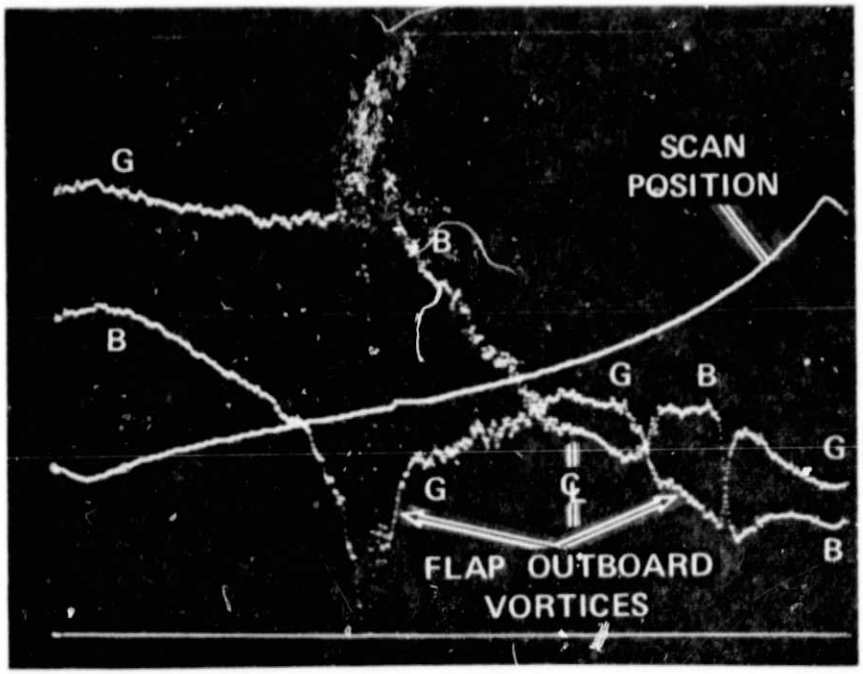


Figure 6.- Boeing 747 wake TCD record. Traverse through flap outboard vortex pair. Note the steep velocity gradient through the left-hand vortex.

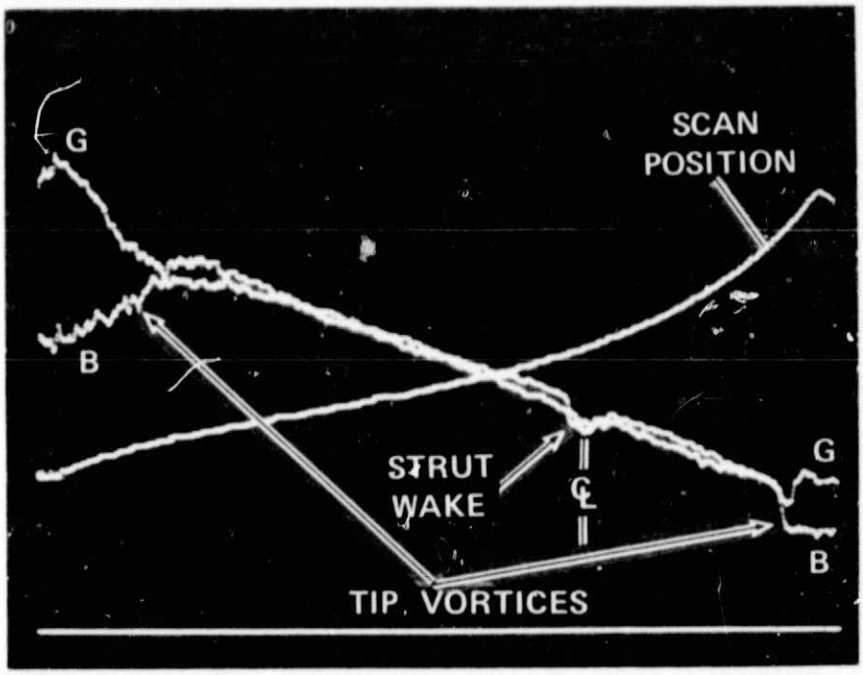


Figure 7.- Boeing 747 wake TCD record. Traverse through the tip vortex pair.

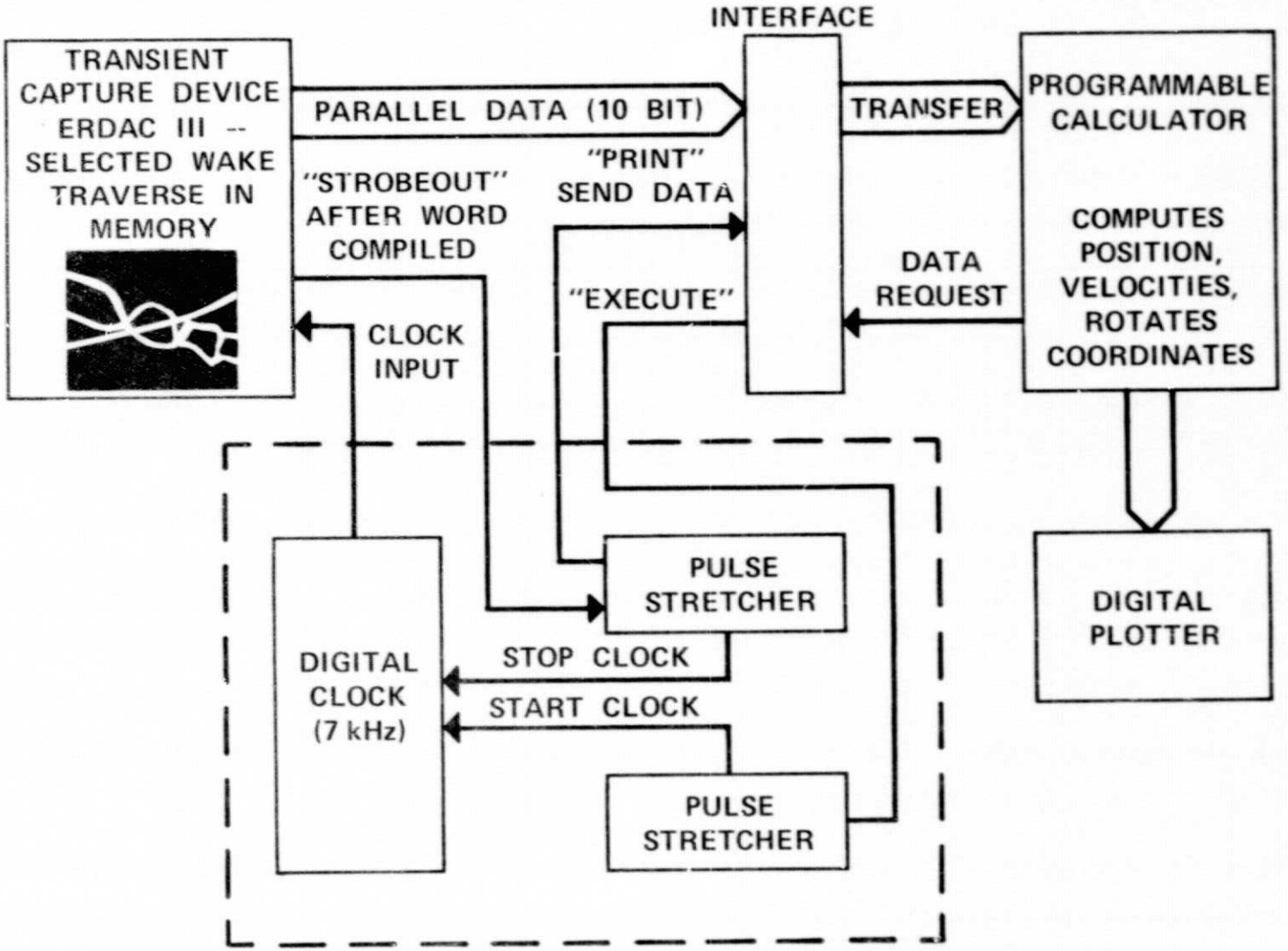


Figure 8.- Data processing and reduction system for the Boeing 747 wake vortex experiment.

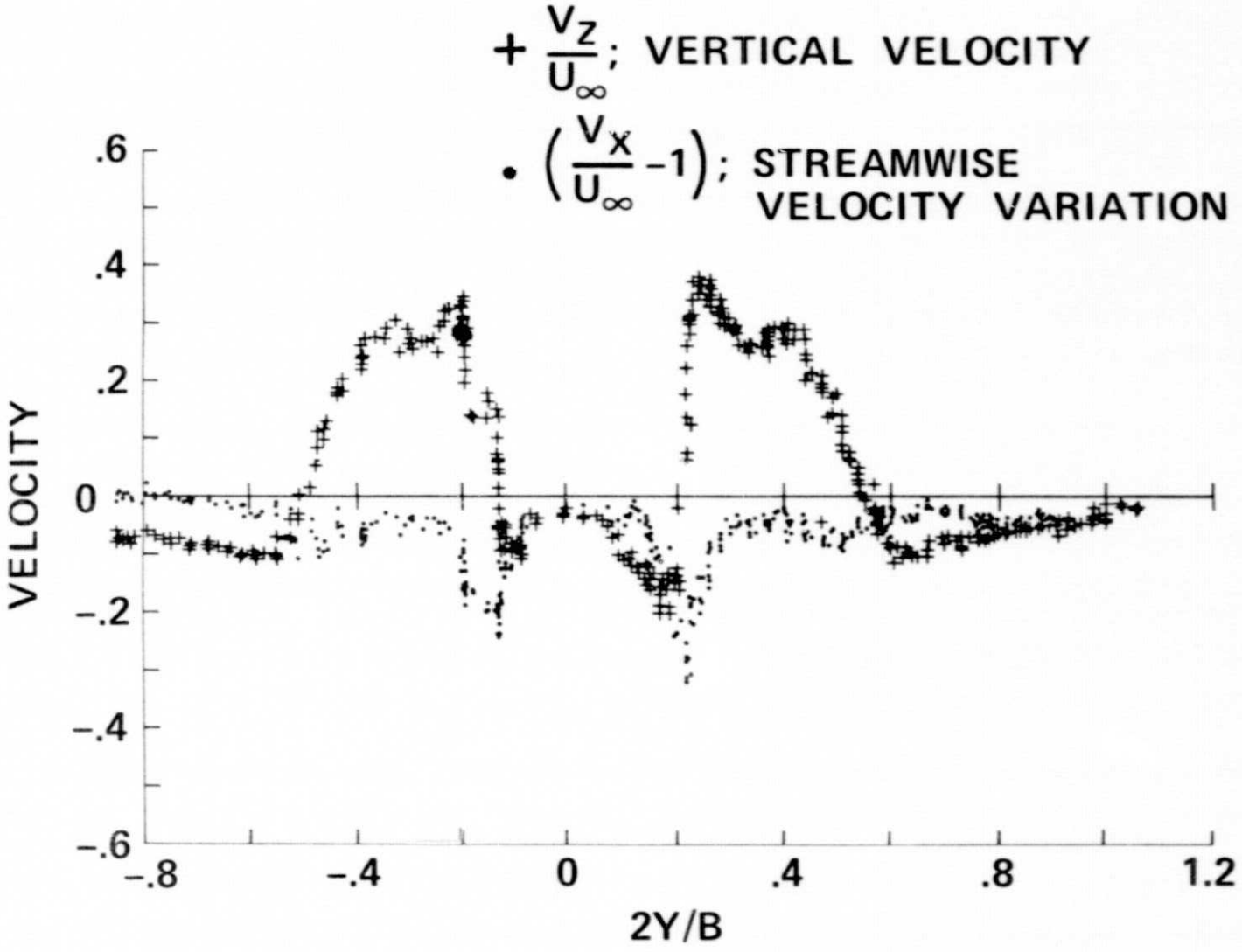


Figure 9.- Processed and plotted data from TCD record of figure 4.

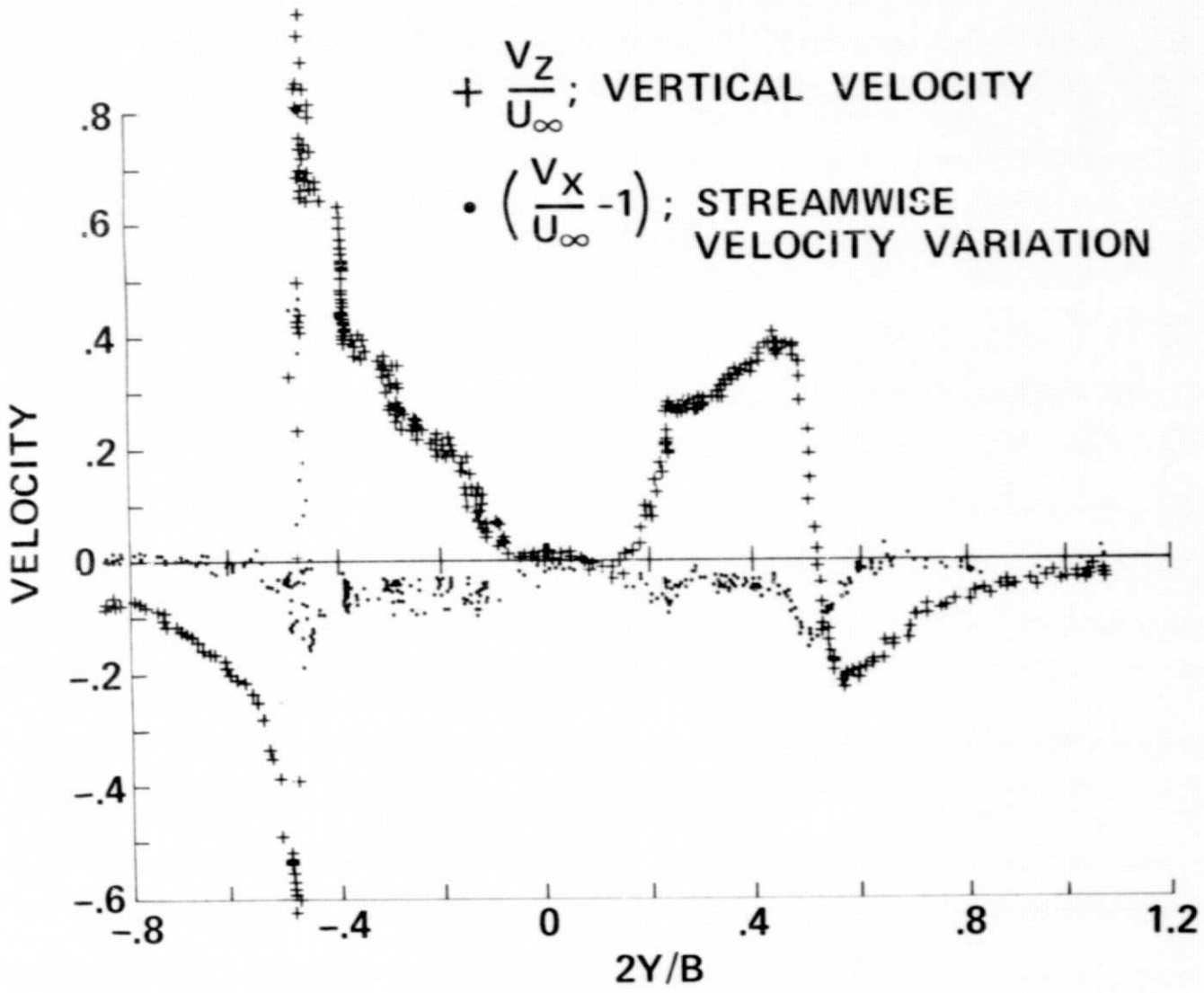


Figure 10.- Processed and plotted data from TCD record of figure 5.

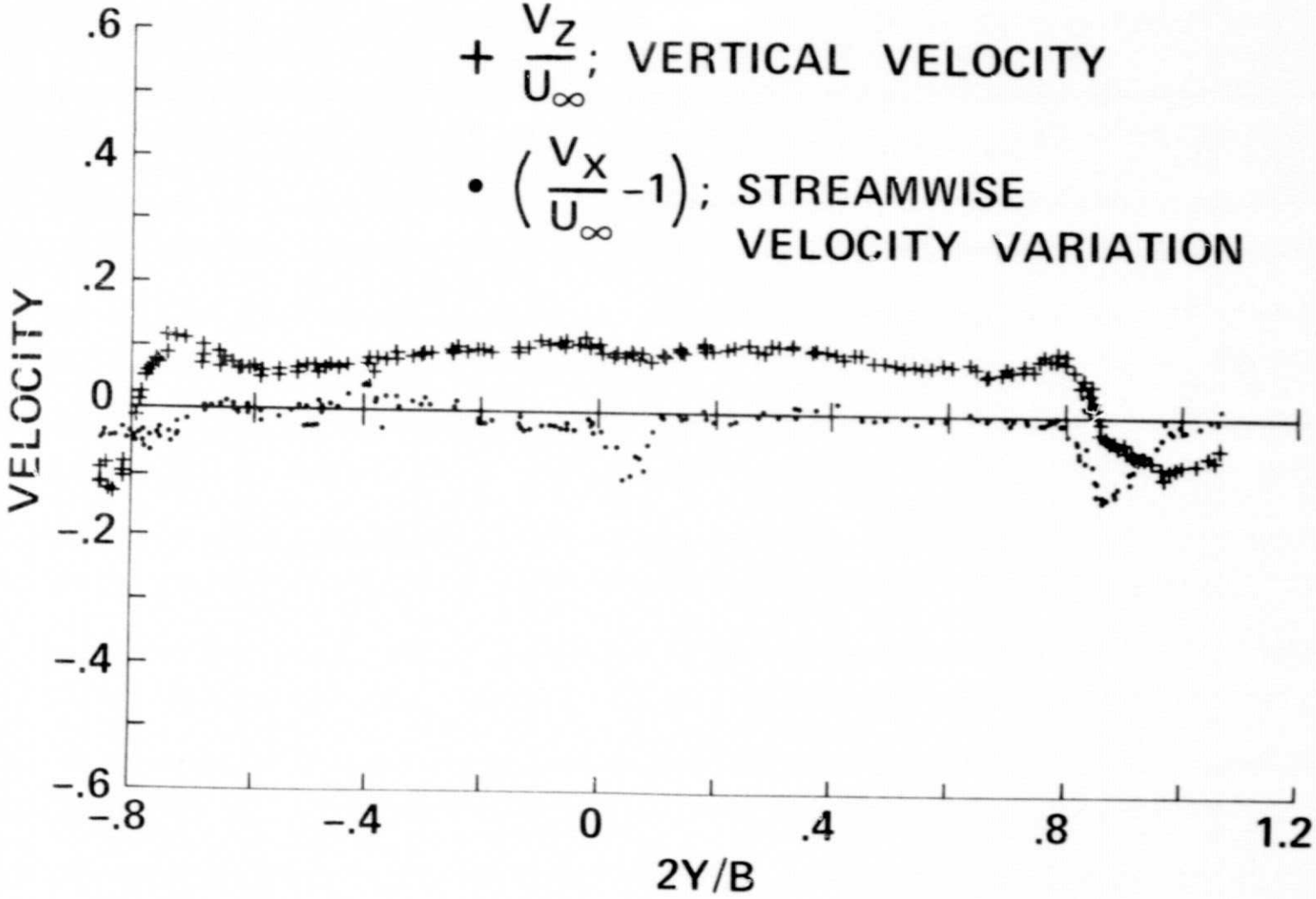


Figure 11.- Processed and plotted data from TCD record of figure 6.

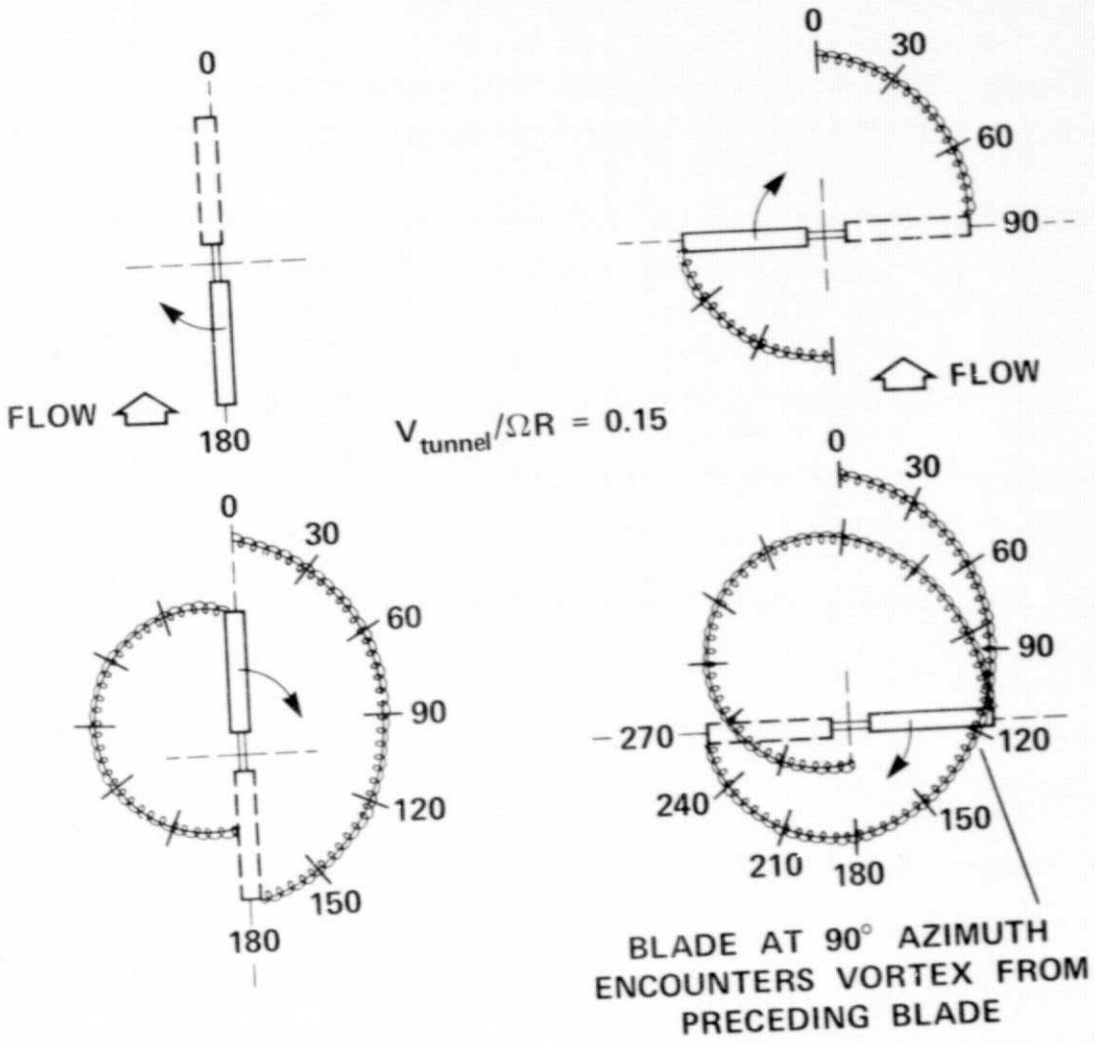


Figure 12.- Instantaneous tip vortex locations for the first four quadrants of rotor rotation.

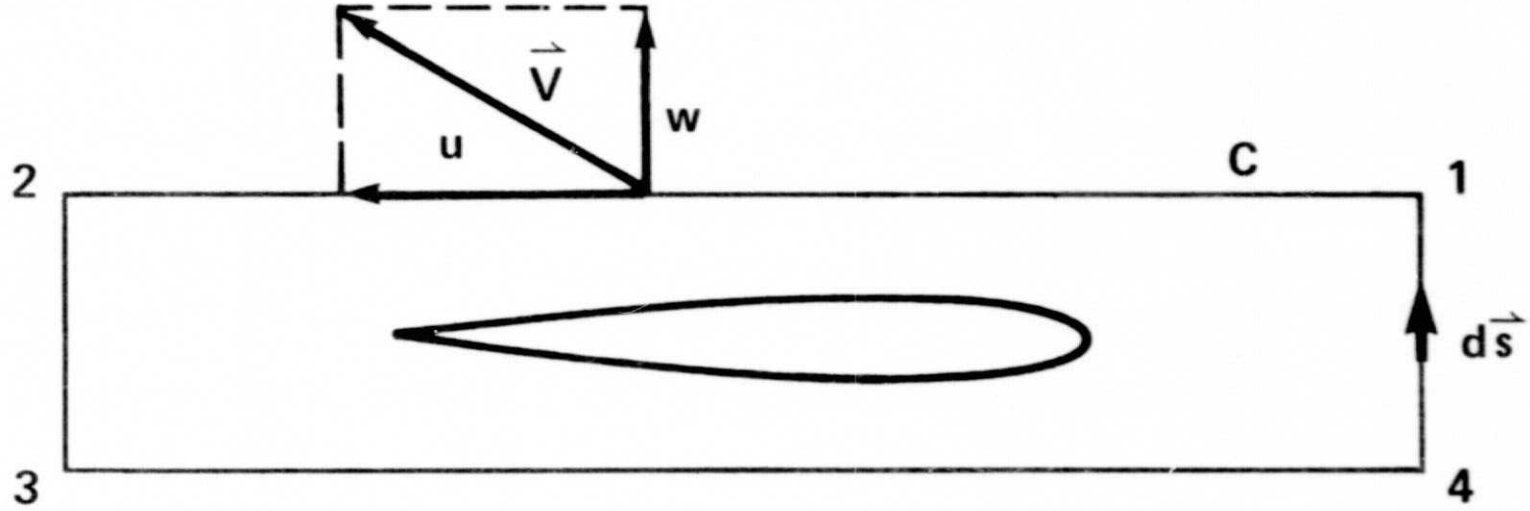


$$\Gamma = \oint_c \vec{V} \cdot d\vec{s}$$

Figure 13.- Survey contour used for determining the bound vorticity (recirculation).

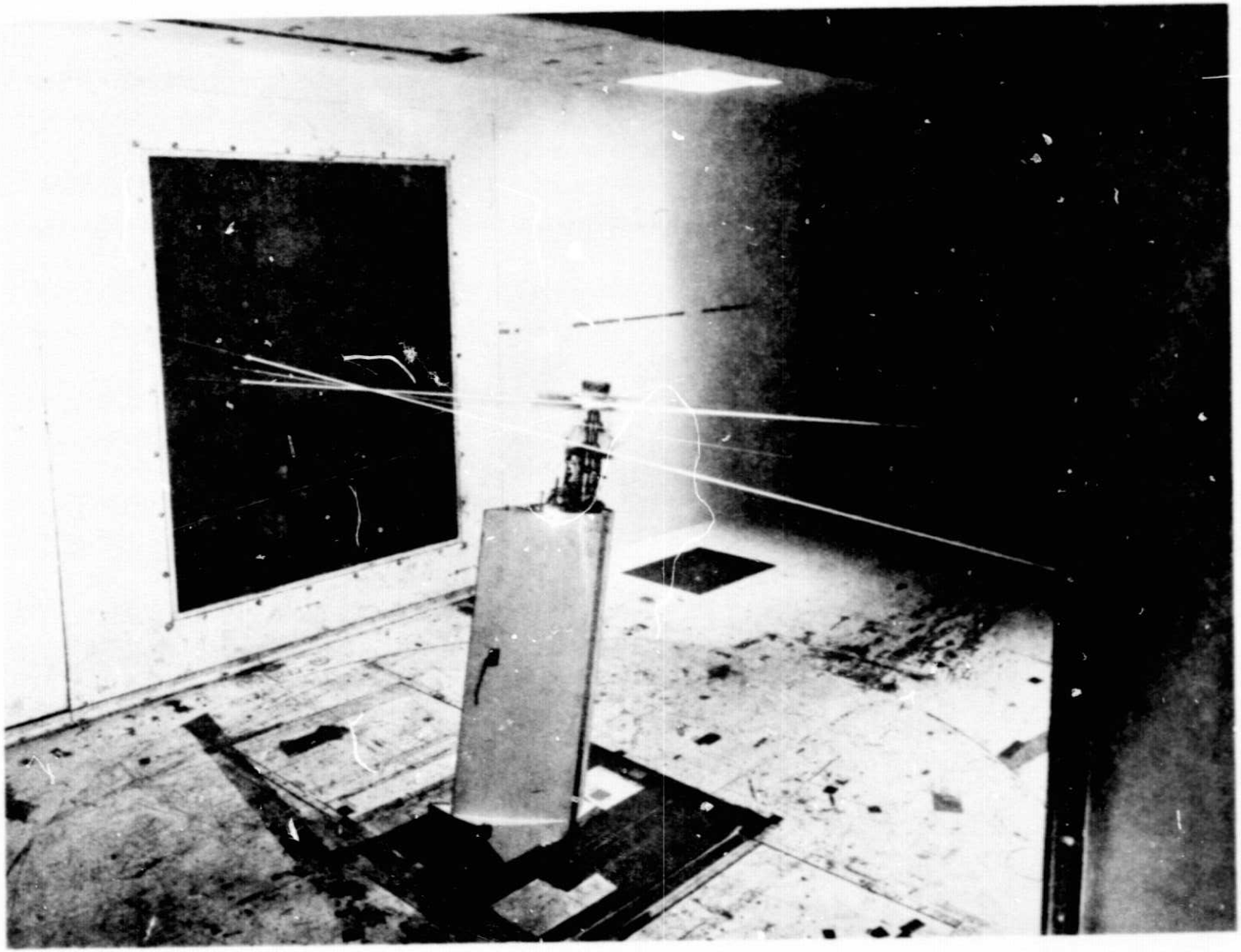

Figure 14.- Photograph of helicopter rotor and laser velocimeter in operation.

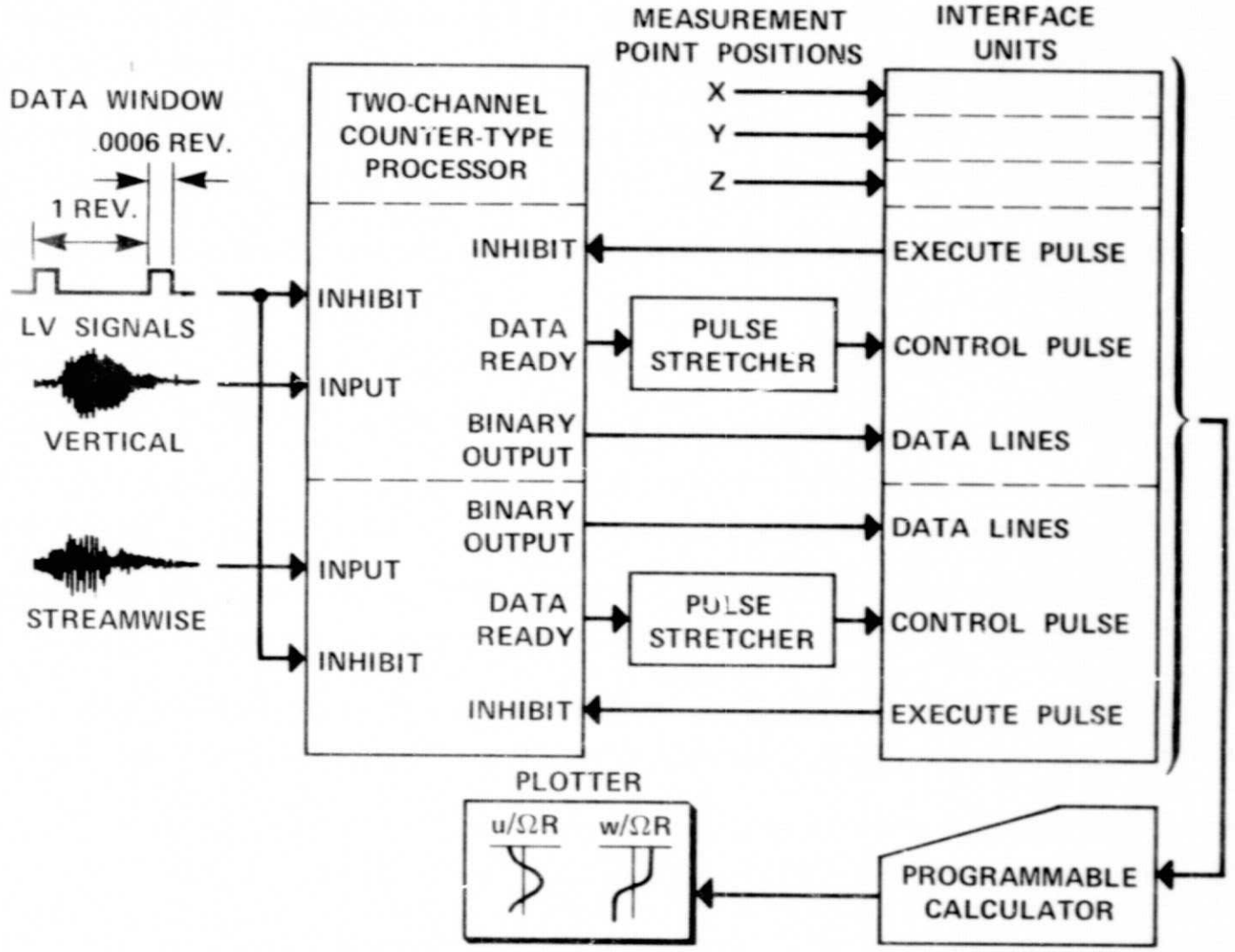


Figure 15.- Schematic diagram of signal processing system for helicopter rotor experiment.

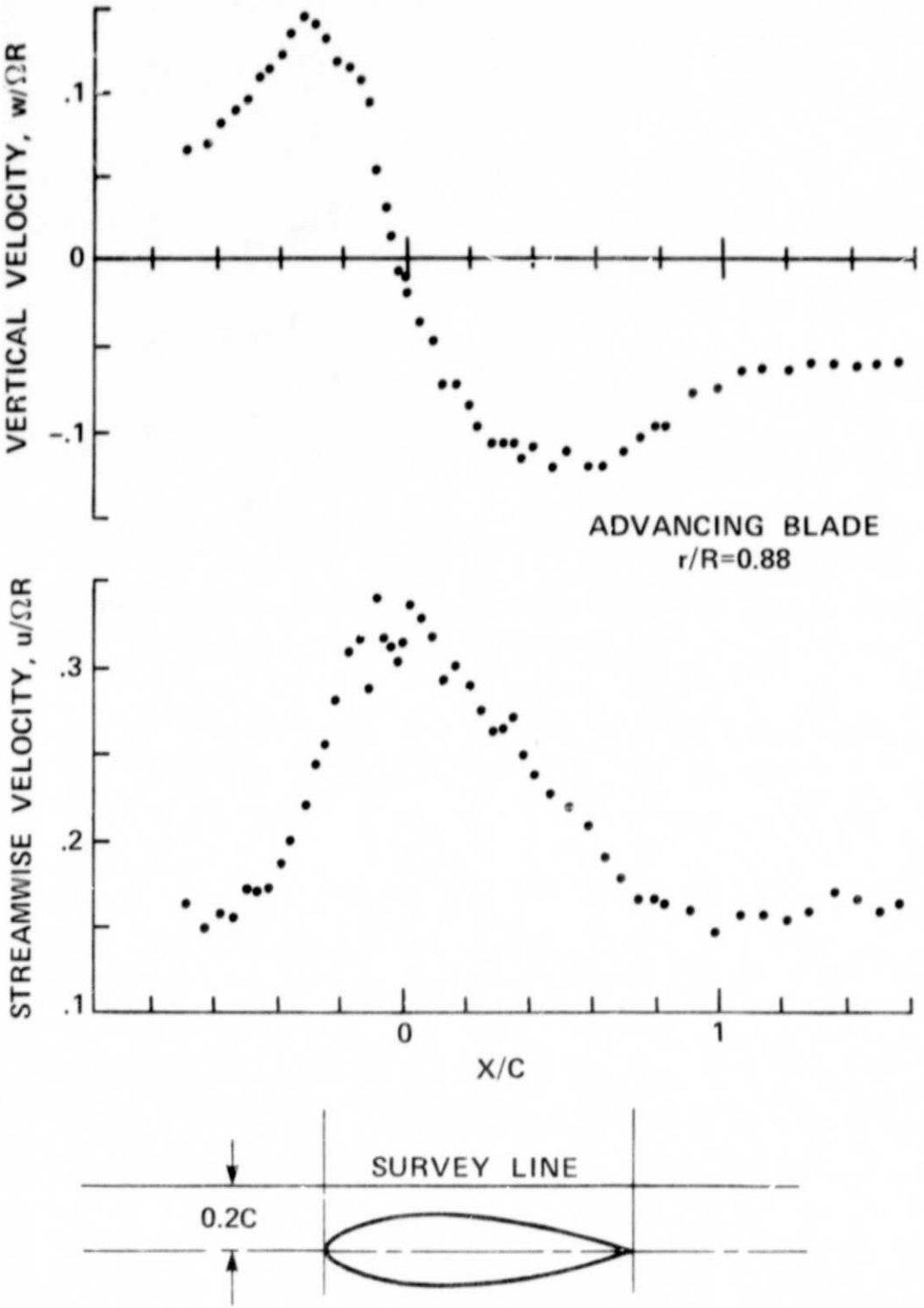


Figure 16.- Velocities above the blade at 90° azimuth; r/R = 0.88.

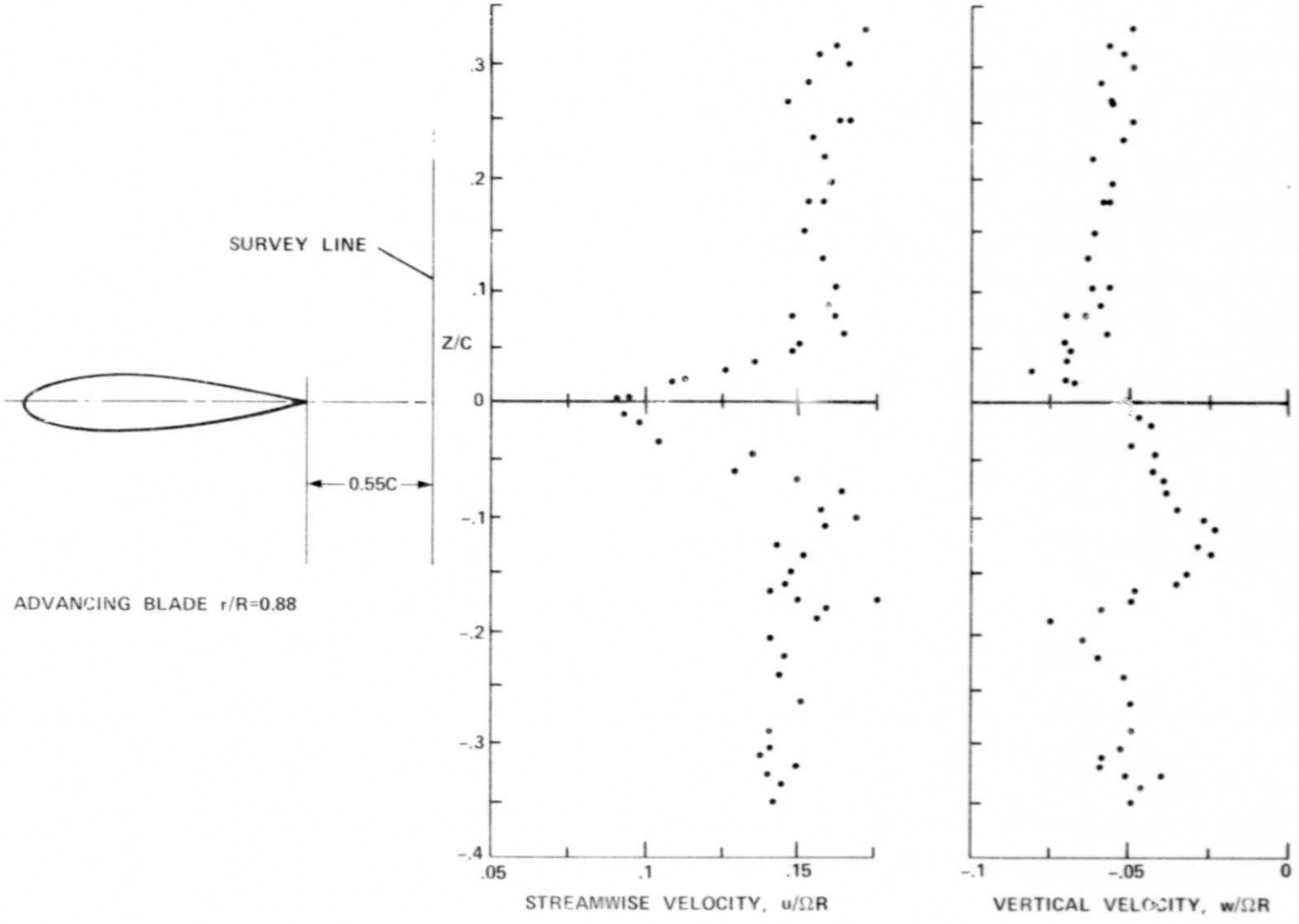


Figure 17.- Velocities behind the blade at 90° azimuth; r/R = 0.88.

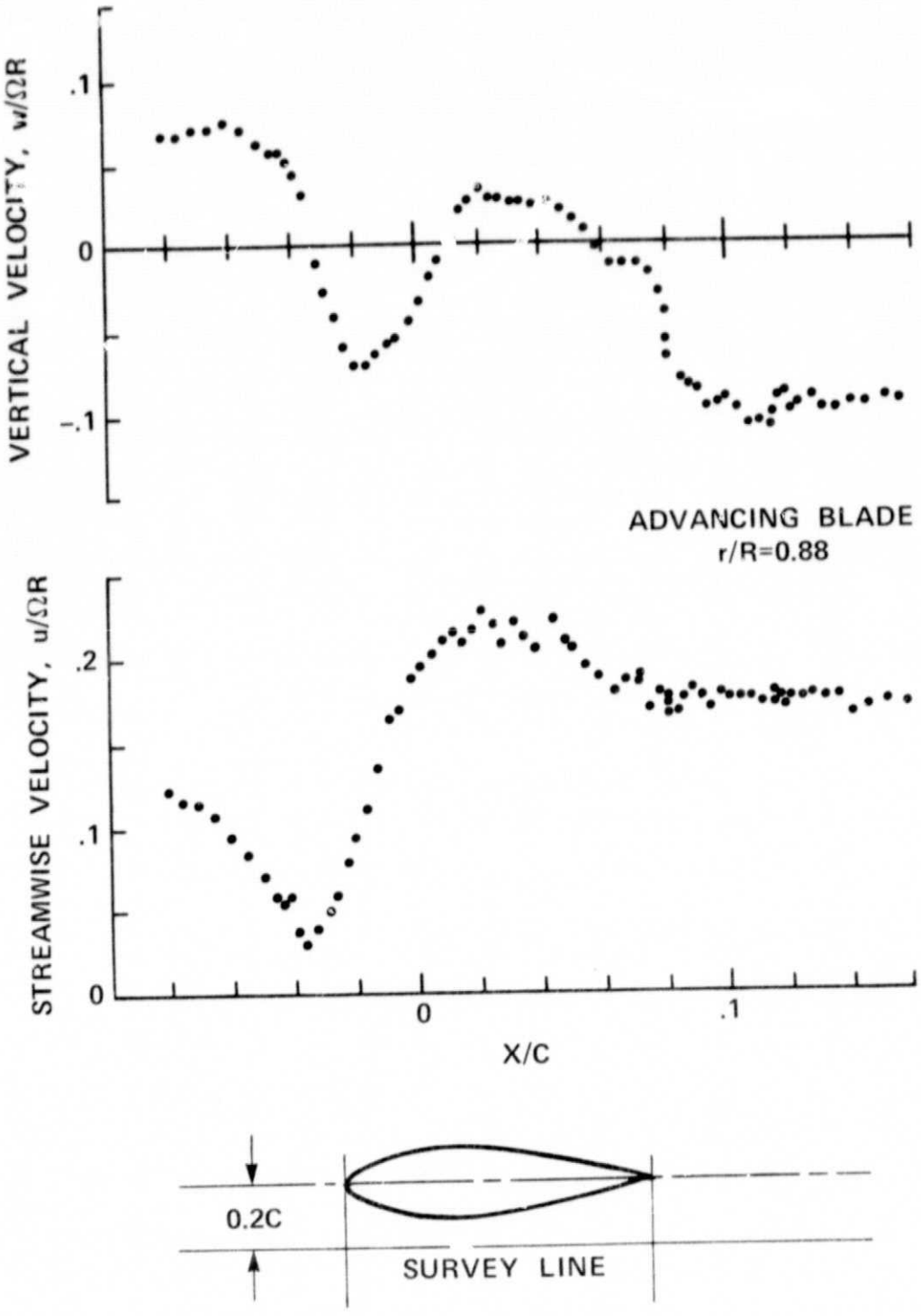


Figure 18.- Velocities below the blade at 90° azimuth; r/R = 0.88.

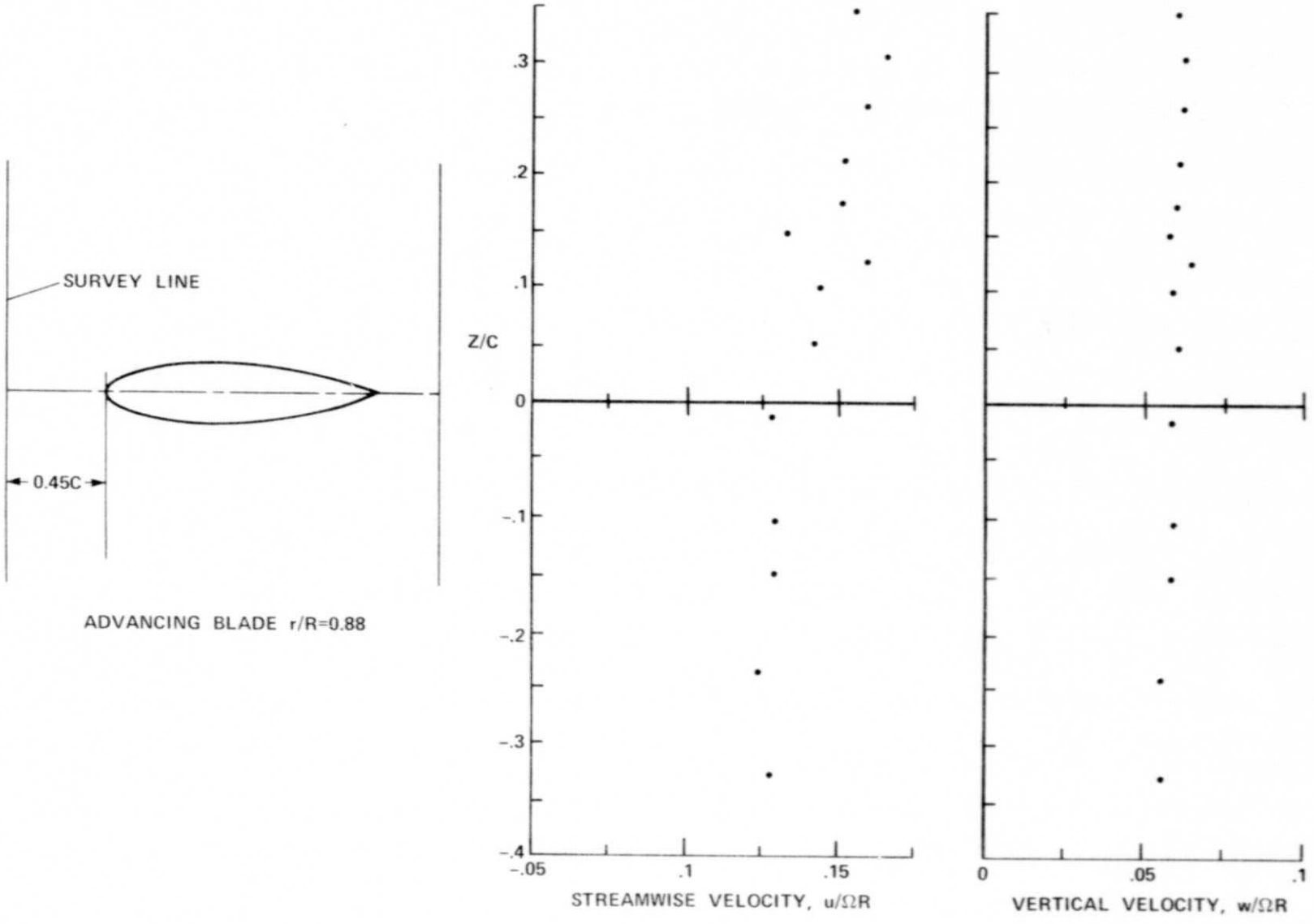


Figure 19.- Velocities ahead of the blade at 90° azimuth; r/R = 0.88.

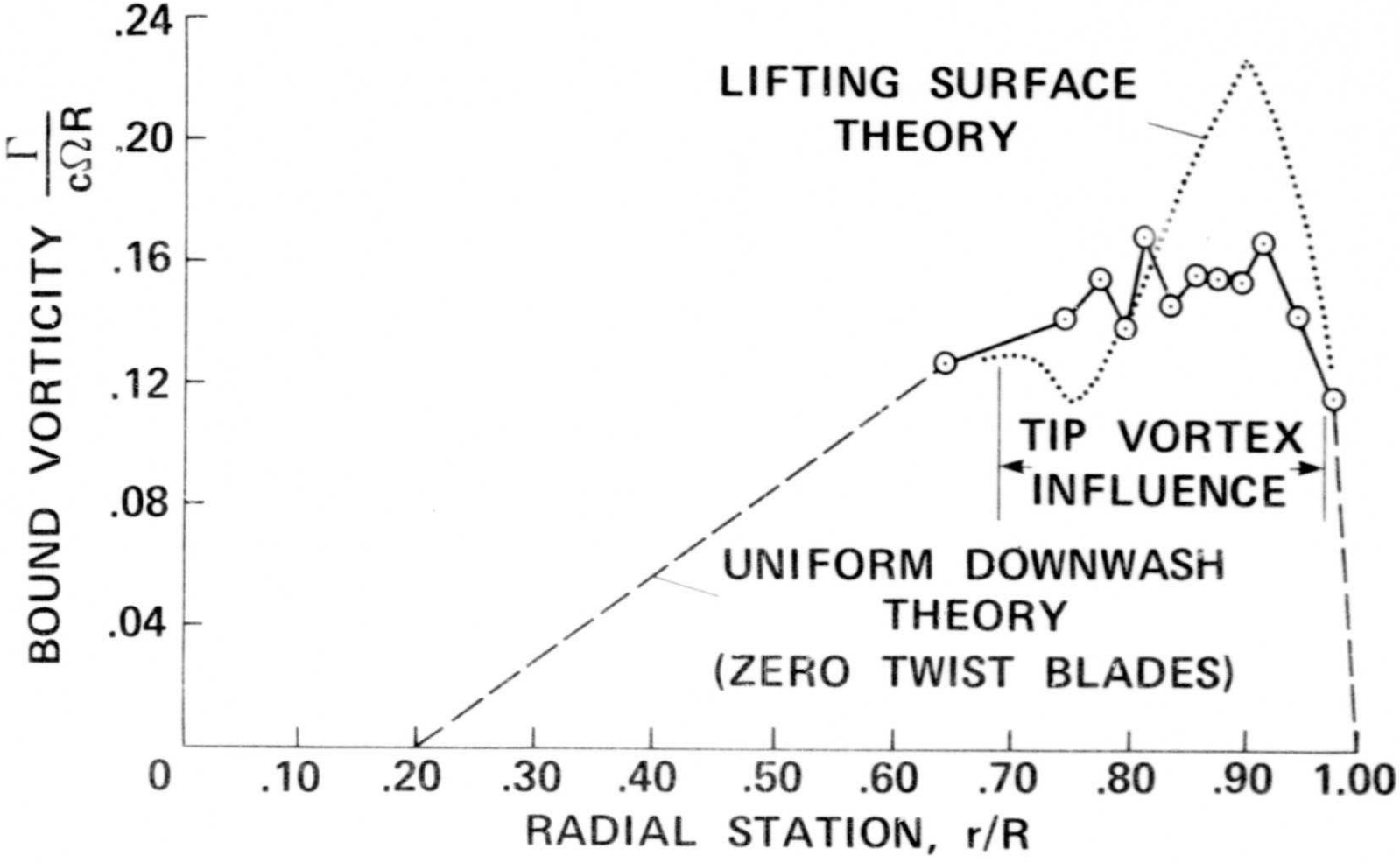


Figure 20.- Distribution of bound vorticity (circulation) along the advancing blade (90° azimuth).